Published for SISSA by Springer

Received: October 21, 2022
Revised: March 1, 2023
Accepted: April 14, 2023
Published: June 22, 2023

Measurement of the Λ_c^+ to D^0 production ratio in peripheral PbPb collisions at $\sqrt{s_{\rm NN}} = 5.02\,\text{TeV}$

The LHCb collaboration

E-mail: benjamin.audurier@llr.in2p3.fr

Abstract: We report on a measurement of the Λ_c^+ to D^0 production ratio in peripheral PbPb collisions at $\sqrt{s_{\rm NN}} = 5.02\,\text{TeV}$ with the LHCb detector in the forward rapidity region $2 < y < 4.5$. The Λ_c^+ (D^0) hadrons are reconstructed via the decay channel $\Lambda_c^+ \to pK^-\pi^+$ ($D^0 \to K^-\pi^+$) for $2 < p_{\rm T} < 8\,\text{GeV}/c$ and in the centrality range of about 65–90%. The results show no significant dependence on $p_{\rm T}$, y or the mean number of participating nucleons. They are also consistent with similar measurements obtained by the LHCb collaboration in pPb and Pbp collisions at $\sqrt{s_{\rm NN}} = 5.02\,\text{TeV}$. The data agree well with predictions from PYTHIA in pp collisions at $\sqrt{s} = 5\,\text{TeV}$ but are in tension with predictions of the Statistical Hadronization model.

Keywords: Charm Physics, Heavy Ion Experiments, Heavy Quark Production, Relativistic Heavy Ion Physics

ArXiv ePrint: 2210.06939

https://doi.org/10.1007/JHEP06(2023)132

JHEP06(2023)132

Contents

JHEP06(2023)132

1 Introduction

Historically, heavy flavor (HF) hadrons (e.g containing at least one c or b quark) have been extensively used to study the deconfined state of hadronic matter, the Quark-Gluon Plasma (QGP) [1–3], in particular at the LHC and RHIC [4–6]. Because their high masses exceed the QCD energy scale, charm and beauty quarks are produced at an early stage of the collision and experience the entire evolution of the colliding medium. Medium-induced energy loss has been studied by measuring the so-called nuclear modification factor ($R_{\rm AA}$), defined as the ratio of the production yield in nucleus-nucleus (AA) collisions to the one in pp collisions scaled by the number of binary nucleon-nucleon collisions. The measurements of the production cross-section, together with studies of the elliptic flow, indicate a strong interaction between heavy quarks and the deconfined medium. In addition, HF hadrons provide a good laboratory to study hadronization. In particular, baryon-to-meson production ratios are of great interest as they are only sensitive to hadronization. Many measurements have been carried on in e^+e^- [7–9] and pp collisions [10–12] to measure fragmentation functions of heavy quarks into heavy hadrons, the latter being extensively used to describe hadron production at high transverse momentum ($p_{\rm T}$). However, recent measurements of the Λ_c^+

to D^0 production ratio[1] ($R_{\Lambda_c^+/D^0}$) challenge understanding of hadronization. At the LHC, ALICE has measured the charmed baryon-to-meson ratio at mid-rapidity in pp, pPb and PbPb collisions at $\sqrt{s} = 7\,\text{TeV}$ and $\sqrt{s_{\text{NN}}} = 5.02\,\text{TeV}$, respectively [13–16]. The measured $R_{\Lambda_c^+/D^0}$ ratio is larger than predictions of the pp event generator PYTHIA 8 [17] with the so-called MONASH tuning for pp data. This tuning does include a color reconnection (CR) mechanism but only at leading order approximation [18], and data can only be explained by the next-to-leading order approximation. In addition, another measurement of $R_{\Lambda_c^+/D^0}$ was carried out by ALICE versus the number of charged particles produced (i.e multiplicity) in pp collisions at $\sqrt{s} = 13$ TeV [19] at mid-rapidity. The results show an evolution of the p_{T} dependence of the ratio as the multiplicity increases, with a shift of the mean p_{T} distribution towards a higher value, while the p_{T}-integrated value of $R_{\Lambda_c^+/D^0}$ remains constant. The PbPb result shows also a large enhancement of the ratio compared to pp and pPb collisions, with a significant dependence of the p_{T} distribution with centrality. Similarly, CMS [20] has performed the same measurement at mid-rapidity in pp and PbPb collisions at $\sqrt{s_{\text{NN}}} = 5.02\,\text{TeV}$, for $p_{\text{T}} > 5\,\text{GeV}/c$ and $p_{\text{T}} > 10\,\text{GeV}/c$, respectively. Compatible results are found between the two data samples for the common range in p_{T} (i.e $p_{\text{T}} > 10\,\text{GeV}/c$). In this case, the data are well described by PYTHIA 8 only when the CR mechanism beyond leading colour approximation is used. At the RHIC collider, the STAR collaboration has also measured $R_{\Lambda_c^+/D^0}$ at mid-rapidity in Au-Au collisions at $\sqrt{s_{\text{NN}}} = 200\,\text{GeV}$ [21]. An enhanced baryon-to-meson ratio is found at low p_{T} compared to scaled pp collisions. It is worth mentioning that both ALICE and STAR measurements in AA collisions can be described by a coalescence hadronization mechanism [6, 22–26] in which quarks can (re)combine with close-by partons in the QGP to form hadrons. Other predictions based on the Statistical Hadronization Model (SHM) [27], using an augmented set of excited charm baryons based on the relativistic quark model (RQM), have successfully described the charmed baryon-to-meson ratio measured at RHIC and LHC. In this model, the relative abundances of the different charm hadron species are fixed by the SHM, while their p_{T} spectra are described using independent fragmentation of charm quarks. Finally, a last class of model based on transport equations, using both fragmentation and coalescence effect, can successfully reproduce the ALICE and RHIC data in nucleus-nucleus collisions [28].

As mentioned, ALICE, CMS, and STAR measure a $R_{\Lambda_c^+/D^0}$ in heavy-ion collisions at mid-rapidity, with a raising trend from low to intermediate transverse momentum. Regardless of the theoretical model used to interpret the data, results at mid-rapidity point toward an effect that depends either on the charged particle multiplicity or the centrality. The latter can be interpreted as a dependence on the mean number of nucleons participating in the collision ($\langle \text{N}_{\text{part}} \rangle$). On the other hand, LHCb has measured a ratio with no p_{T} dependence in pPb collisions at $\sqrt{s_{\text{NN}}} = 5.02\,\text{TeV}$ in the rapidity (p_{T}) range $2 < y < 4.5$ ($2 < p_{\text{T}} < 8\,\text{GeV}/c$) [29]. These results correspond to smaller $R_{\Lambda_c^+/D^0}$ values compared to measurements by other experiments and are fully compatible with predictions from cold nuclear matter effects [30, 31] within the HELAC-Onia approach [32–34]. The LHCb re-

[1] If not stated otherwise, charge conjugation is assumed throughout the article.

JHEP06(2023)132

sults are yet to be compared with a coalescence-based model. These differences between mid and forward rapidity results indicate a strong rapidity dependence of this ratio and motivate further studies to better improve the model predictions in different phase-space regions.

This paper presents the first measurement of $R_{\Lambda_c^+/D^0}$ production cross-section ratio in the forward rapidity region in peripheral PbPb collisions at $\sqrt{s_{\rm NN}} = 5.02\,\text{TeV}$ by the LHCb collaboration. The paper is organized as follows. Section 2 briefly presents the detector and the data sample. Section 3 describes the analysis steps, from the signal extraction to the estimation of efficiency corrections. The sources of systematic uncertainties are given in section 4. The results are presented and compared to theory predictions in section 5, and conclusions are summarized in section 6.

2 Detector and data selection

The LHCb detector [35, 36] is a single-arm forward spectrometer covering the pseudorapidity range $2 < \eta < 5$, designed for the study of particles containing b or c quarks. The detector includes a high-precision tracking system consisting of a silicon-strip vertex detector (VELO) surrounding the interaction region [37], a large-area silicon-strip detector located upstream of a dipole magnet (UT) with a bending power of about 4 Tm, and three stations of silicon-strip detectors and straw drift tubes [38] placed downstream of the magnet. The tracking system provides a measurement of the momentum, p, of charged particles with a relative uncertainty that varies from 0.5% at low momentum to 1.0% at 200 GeV/c. The minimum distance of a track to a primary collision vertex (PV), the impact parameter (IP), is measured with a resolution of $(15 + 29/p_{\rm T})\,\mu$m, with $p_{\rm T}$ in GeV/c. Different types of charged hadrons are distinguished using information from two ring-imaging Cherenkov detectors [39]. Photons, electrons and hadrons are identified by a calorimeter system consisting of scintillating-pad and preshower detectors (SPD), an electromagnetic (ECAL) and a hadronic (HCAL) calorimeter. Muons are identified by a system composed of alternating layers of iron and multiwire proportional chambers [40]. The online event selection is performed by a trigger [41], which consists of a hardware stage, based on information from the calorimeter and muon systems, followed by a software stage, which applies a full event reconstruction.

The PbPb collision data at $\sqrt{s_{\rm NN}} = 5.02\,\text{TeV}$ were recorded in 2018 and correspond to an integrated luminosity of about $210\,\mu\text{b}^{-1}$. Offline quality selections are applied on a run-by-run basis, based on the trend of trigger counts with time. At the hardware trigger stage, events containing Λ_c^+ or D^0 candidates are required to match the minimum bias (MB) trigger corresponding to a requirement of at least four SPD hits or a high-$p_{\rm T}$ muon ($p_{\rm T} > 10\,\text{GeV}/c$) or a minimal energy deposit in HCAL ($E_{\rm T} > 15\,\text{GeV}/c$). The events are required to have at least 15 VELO tracks in the backward direction and the number of clusters (Nc) in the VELO should be at least 1000; these requirements suppress contamination from both the Pb-gas[2] and ultra-peripheral collisions. The latter are defined

[2]Simultaneously to PbPb collisions, Neon gas was injected in the beam pipe near the interaction point, using the LHCb fixed-target SMOG system [42].

JHEP06(2023)132

as electromagnetic nucleus-nucleus interactions where the impact parameter (b) is greater than the sum of the nuclei radii. Finally, events are rejected if $N_c \geq 10000$, due to hardware limitations.

The Λ_c^+ (D^0) candidates are reconstructed via the decay channel $\Lambda_c^+ \to pK^-\pi^+$ ($D^0 \to K^-\pi^+$), with a selection on transverse momentum $2 < p_{\mathrm{T}} < 8$ GeV/c and rapidity $2 < y < 4.5$. Offline selections are applied to the candidates following the same strategy as in pPb collisions [43] to ensure a high signal significance and improve the purity of the D^0 and Λ_c^+ candidates. Pion, kaon, and proton tracks should match tracking and particle identification (PID) quality requirements. The Λ_c^+ (D^0) decay products are required to have $p_{\mathrm{T}} > 400\,\mathrm{MeV}/c$ ($p_{\mathrm{T}} > 500\,\mathrm{MeV}/c$) and $2 < y < 4.5$. The charm hadron lifetime is required to be less than 0.3 ps to reduce the fraction of non-prompt contribution coming from b-hadron decay. The cosine of the direction angle between the candidate's momentum and the vector between the PV and the candidate's decay vertex, is required to be larger than 0.9998. In addition, a fiducial cut around the beams' collision point is applied based on the primary vertex (PV) of the Λ_c^+ and D^0 candidates.

Simulated PbPb collisions at $\sqrt{s_{\mathrm{NN}}} = 5.02\,\mathrm{TeV}$ with full event reconstruction are used to evaluate efficiencies. The Λ_c^+ and D^0 candidates are generated with PYTHIA 8 [17] and embedded into minimum bias PbPb collisions from the EPOS event generator [44] tuned with LHC data [45]. Decays of hadronic particles are described by EvtGen [46], in which final-state radiation is generated using PHOTOS [47]. The interaction of the generated particles with the detector, and its response, are implemented using the Geant4 toolkit [48, 49] as described in ref. [50].

3 Analysis overview

The $R_{\Lambda_c^+/D^0}$ ratio is obtained through the ratio of corrected yields as:

$$R_{\Lambda_c^+/D^0}(p_{\mathrm{T}}, y \text{ or } \langle \mathrm{N_{part}} \rangle) = \frac{\mathcal{B}^{D^0 \to K^-\pi^+}}{\mathcal{B}^{\Lambda_c^+ \to pK^-\pi^+}} \frac{Y^{\Lambda_c^+}(p_{\mathrm{T}}, y \text{ or } \langle \mathrm{N_{part}} \rangle)}{Y^{D^0}(p_{\mathrm{T}}, y \text{ or } \langle \mathrm{N_{part}} \rangle)}, \tag{3.1}$$

where $\mathcal{B}^{D^0} = (3.950 \pm 0.031)\%$ ($\mathcal{B}^{\Lambda_c^+} = (6.28 \pm 0.32)\%$) is the branching fraction for the D^0 (Λ_c^+) decay channel [51], respectively; p_{T} and y are the transverse momentum and rapidity of the D^0 (Λ_c^+) candidate; $\langle \mathrm{N_{part}} \rangle$ is the mean number of nucleons participating in the collision and is related to the centrality of the collision; Y^{D^0} ($Y^{\Lambda_c^+}$) is the D^0 (Λ_c^+) corrected yield defined as

$$Y^{D^0,\Lambda_c^+}(p_{\mathrm{T}}, y \text{ or } \langle \mathrm{N_{part}} \rangle) = \frac{N^{D^0,\Lambda_c^+}(p_{\mathrm{T}}, y \text{ or } \langle \mathrm{N_{part}} \rangle) \cdot f_{\mathrm{prompt}}^{D^0,\Lambda_c^+}(p_{\mathrm{T}}, y \text{ or } \langle \mathrm{N_{part}} \rangle)}{\epsilon_{\mathrm{tot}}^{D^0,\Lambda_c^+}(p_{\mathrm{T}}, y \text{ or } \langle \mathrm{N_{part}} \rangle)}. \tag{3.2}$$

In eq. (3.2), N^{D^0,Λ_c^+} is the inclusive number of particles measured in the PbPb dataset, and $f_{\mathrm{prompt}}^{D^0,\Lambda_c^+}$ is the fraction of particles produced promptly in PbPb collisions, while ϵ_{tot} is defined as the total efficiency (see section 3.3). Finally, $\langle \mathrm{N_{part}} \rangle$ is defined as the mean number of nucleons participating in the collision. A brief description of the method used to evaluate this quantity is given in section 3.1.

JHEP06(2023)132

N_c interval	$\langle \mathrm{N_{part}} \rangle$	σ_{part}
1000–10000	15.8	10.0
1000–3000	6.5	2.5
3000–5500	12.4	4.4
5500–10000	26.6	7.5

Table 1. values of $\langle \mathrm{N_{part}} \rangle$ in N_c intervals, with σ_{part} indicating the total systematic uncertainty of $\langle \mathrm{N_{part}} \rangle$.

3.1 Centrality determination

In heavy-ion collisions, centrality classes are defined as percentiles of the total inelastic hadronic PbPb cross-section and are related to the impact parameter b of the collision: the more central (peripheral) the collision, the smaller (greater) the b value, and the smaller (greater) the centrality percentile. Likewise, $\langle \mathrm{N_{part}} \rangle$ increases from peripheral to central collisions. The Glauber Monte Carlo (GMC) model [52] is used to estimate all these geometrical quantities from recorded data. A detailed description of the centrality estimation in the LHCb experiment can be found in ref. [53]. The method is based on a binned fit of the total energy deposit in ECAL with the GMC model in MB data, collected with the same trigger conditions as that of the signal sample. Once the fit is performed, a centrality table is produced, mapping the total ECAL energy deposit and $\langle \mathrm{N_{part}} \rangle$.

While the recorded data sample used to fit the GMC model covers the full centrality range, data used to compute $R_{\Lambda_c^+/D^0}$ are limited to $N_c < 10^4$ and centrality at about 65−90%. A one-to-one correspondence between ECAL and the geometrical quantity is performed on an event-by-event basis using the GMC model. Data are divided into three intervals in N_c (1000–3000, 3000–5500 and 5500–10000), based on the statistics available from the signal extraction. For each interval, other quantities (e.g. $\langle \mathrm{N_{part}} \rangle$) are derived. A lower cut on N_c and on the total deposited ECAL energy to be above 310 MeV are applied to exclude the centrality range 90–100% where most of the electromagnetic contamination occurs, which could bias the data. Results are given in table 1. Three sources of systematic uncertainty associated with $\langle \mathrm{N_{part}} \rangle$ of each interval are considered: (i) the reference hadronic cross-section parameter; (ii) the fit uncertainty; (iii) the bin size uncertainty. These uncertainties are summed in quadrature to compute the total systematic uncertainty presented in table 1.

3.2 Signal extraction

The signal extraction is performed after the selection criteria listed in section 2 are applied. Figure 1 shows the (top) $K^-\pi^+$ and (bottom) $pK^-\pi^+$ invariant-mass spectra for the selected D^0 and Λ_c^+ candidates, respectively. The data are fitted using unbinned maximum-likelihood fits combining a Crystal Ball (CB) function [54] for the signal, and a first-order polynomial function for the background. While the CB function is chosen as it models the radiative tail of the invariant mass peak, the first-order polynomial function is chosen empirically to describe the observed background. The mean and width of the CB

JHEP06(2023)132

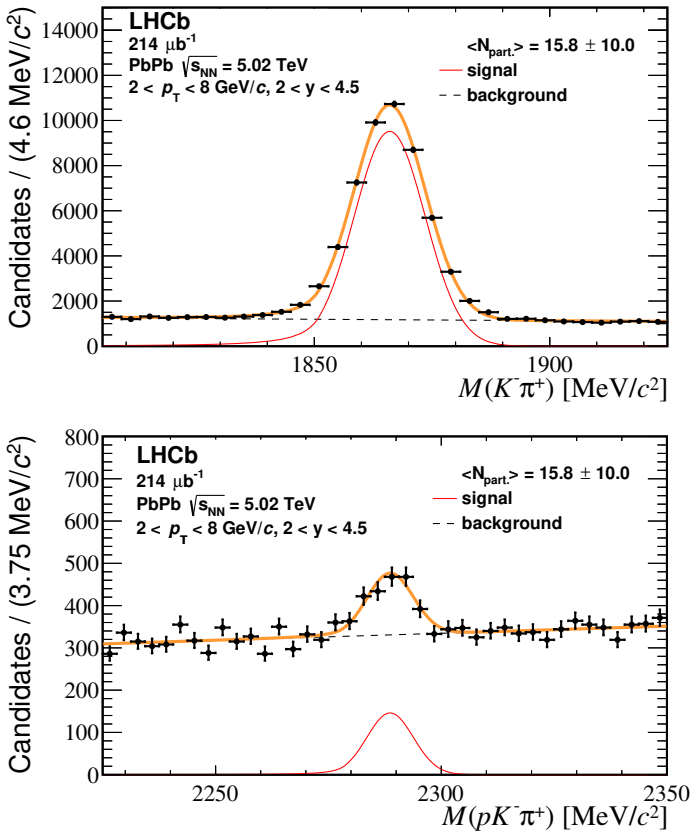

Figure 1. Invariant-mass spectra of (top) $K^-\pi^+$ and (bottom) $pK^-\pi^+$ final states. The data are overlaid with the results of the fit.

function are left free, while the other parameters are fixed to the values extracted from the simulation. An alternative used to assess systematic uncertainty for the background description is to multiply the first-order polynomial by an exponential function. The total number of fitted D^0 (Λ_c^+) signal yield is 46000 (600) events.

To estimate the fraction of prompt D^0 (Λ_c^+) hadrons in the measured yield, the background contribution is first subtracted from the datasets using the *sPlot* technique [55]. A fit to the $\log(\chi^2_{\rm IP})$ distribution of the signal is performed to discriminate the prompt from non-prompt contributions. The $\chi^2_{\rm IP}$ is defined as the difference in the vertex-fit χ^2 of a given PV reconstructed with and without the candidate under consideration. An example of such fit is given in figure 2, where the $\log(\chi^2_{\rm IP})$ distributions are fitted with a CB (Gaussian) function for the prompt (non-prompt) component. It is worth noticing that the $\log(\chi^2_{\rm IP})$ is a better prompt/non-prompt discriminant for D^0 candidates when compared to Λ_c^+ candidates. This is due to the shorter lifetime of the Λ_c^+ baryon: for non-prompt candidates, typically the addition of the Λ_c^+ track to the PV fit leads to a lower value of $\chi^2_{\rm IP}$ than that of the non-prompt D^0 track.

JHEP06(2023)132

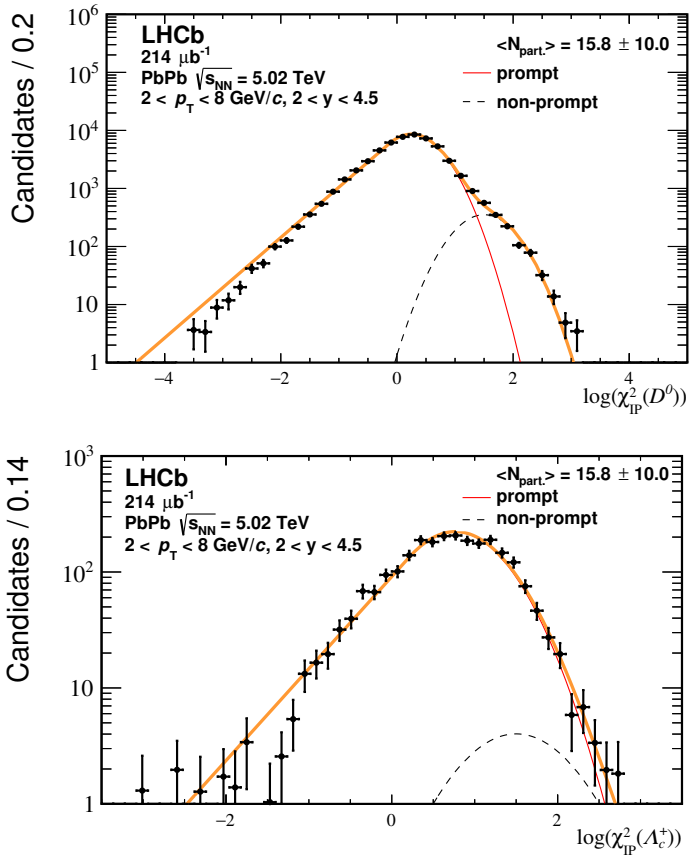

Figure 2. Distributions of $\chi^2_{\rm IP}$ of the D^0 (top) and Λ_c^+ (bottom) after background substraction. The data are overlaid with the results of the fit.

3.3 Efficiency estimation

The total efficiency ($\epsilon_{\rm tot}$) is factorized as

$$\epsilon_{\rm tot}^{D^0,\Lambda_c^+}(p_{\rm T}, y \text{ or } N_c) = \epsilon_{\rm acc}^{D^0,\Lambda_c^+}(p_{\rm T}, y) \times \epsilon_{\rm rec\&sel}^{D^0,\Lambda_c^+}(p_{\rm T}, y \text{ or } N_c) \times \epsilon_{\rm PID}^{D^0,\Lambda_c^+}(p_{\rm T}, y \text{ or } N_c), \quad (3.3)$$

where $\epsilon_{\rm acc}$ is the acceptance; $\epsilon_{\rm rec\&sel}$ is the reconstruction and selection efficiency; $\epsilon_{\rm PID}$ is the PID selection efficiency; $(N_c, p_{\rm T}, y)$ indicate given ranges in N_c, $p_{\rm T}$ and rapidity.

The acceptance $\epsilon_{\rm acc}$, for both Λ_c^+ and D^0 hadrons, is defined as

$$\epsilon_{\rm acc}^{D^0,\Lambda_c^+}(p_{\rm T}, y) = \frac{N_{\rm cand}^{2<y<4.5}}{N_{\rm cand}^{\rm fid}}, \quad (3.4)$$

where $N_{\rm cand}^{\rm fid}$ are simulated D^0 or Λ_c^+ yields within the fiducial acceptance and $N_{\rm cand}^{2<y<4.5}$ indicate the number of the candidates in the fiducial acceptance and having their decay products' rapidity within $2 < y < 4.5$. The fiducial acceptance is defined as $2 < y < 4.5$ and $2 < p_{\rm T} < 8\,{\rm GeV}/c$. This factor is directly computed from simulation based on PYTHIA 8.

JHEP06(2023)132

N_c interval	$k(N_c)$
1000–4000	0.97 ± 0.03
4000–5500	0.93 ± 0.04
5500–10000	0.91 ± 0.05

Table 2. Value of the k factor in intervals of N_c. The uncertainties are obtained from the statistical uncertainties of the different D^0 calibration samples in data and MC summed in quadrature.

The reconstruction and selection efficiency $\epsilon_{\text{rec\&sel}}$, for both Λ_c^+ and D^0 particles, is defined as:

$$\epsilon_{\text{rec\&sel}}^{D^0,\Lambda_c^+}(p_{\text{T}}, y \text{ or } \text{N}_\text{c}) = \frac{\text{N}_{\text{cand}}^{\text{rec.\&sel.}}}{\text{N}_{\text{cand}}^{2<\text{y}<4.5}}, \tag{3.5}$$

where $N_{\text{cand}}^{\text{rec.\&sel.}}$ are reconstructed D^0 and Λ_c^+ candidates passing the selection criteria within the simulation samples. We recall that the samples are produced with the PYTHIA 8 hard processes embedded into generated MB EPOS events. Several sources of bias are considered for $\epsilon_{\text{rec\&sel}}$ due to the limitations of MC to fully model all the bias in the real detector's response. The first source is the tracking algorithm efficiency, defined as the efficiency to reconstruct a track, for which simulations are usually better than in data. Rather than directly measuring the tracking efficiency, the ratio of the efficiency between data and simulation is estimated using two D^0 calibration channels ($D^0 \to K^-\pi^+$ and $D^0 \to K^-\pi^+\pi^-\pi^+$). Their yields are evaluated in PbPb data and simulation and the difference of their ratio from unity is encoded in a factor k. Results are given in table 2. Other sources of systematic uncertainty are the *ab-initio* assumptions on the p_{T}, y and N_c distributions, and correlation effects between these variables not accounted for with the embedding technique. To account for all these effects, an iterative method based on data is employed. In the first step, the raw (i.e not corrected for inefficiency) p_{T}, rapidity, and N_c distributions are extracted from the data based on the signal extraction defined in section 3.2. In the second step, these distributions are corrected using the data-to-simulation tracking efficiency (k factor) and the PID efficiency (ϵ_{PID}) computed with the raw kinematic distributions reconstructed in the simulation. In the third step, the reconstructed distributions from the simulation are weighted using several iterations until they match the data as a function of p_{T}, y, and N_c simultaneously. Finally, $\epsilon_{\text{rec\&sel}}$ is computed in step four. Steps two to four are repeated until $\epsilon_{\text{rec\&sel}}$ converges to a final value, which is the case after three iterations.

The PID efficiency ϵ_{PID} is computed using the weighted simulation samples. The methodology is similar to that used for pp collisions [56], and is based on a tag-and-probe technique. In this approach, the ϵ_{PID} for a given probe particle $\epsilon_{\text{PID}}^{\text{part}}$ (e.g. pion) is computed from a reference sample (e.g. $D^0 \to K^-\pi^+$) where a tight selection cut on the tag particle (i.e. the kaon) is applied, while no PID selection is applied to the probe particle. In the next step, the *sPlot* technique [55] is used to remove the background with the invariant mass as a discriminating variable. Finally, the PID efficiency of the probe is computed as the fraction of candidates (i.e. D^0) fulfilling given PID requirement.

Kaon and pion PID efficiencies are computed using the PbPb D^0 sample, while the proton efficiency is computed from $\Lambda \to \pi^- p$ decays in PbPb data. Two-dimensional maps

JHEP06(2023)132

are then computed for each particle (i.e kaon, pion, proton) as a function of p and y, for different ranges in N_c. Finally, these maps are used to compute hadron PID efficiency for D^0 and Λ_c^+ candidates as

$$\epsilon_{\rm PID}^{D^0,\Lambda_c^+}(p_{\rm T}, y \text{ or } N_c) = \frac{\prod_{\rm part}^{\rm candidate} \epsilon_{\rm PID}^{\rm part}(p, y, N_c)}{N_{\rm cand}^{\rm rec.\&sel.}}, \tag{3.6}$$

where $(p_{\rm T}, y \text{ or } N_c)$ are the candidates kinematic variables and $\epsilon_{\rm PID}^{\rm part}(p, y, N_c)$ is the single-particle efficiency given as functions of the decay products kinematic variables.

4 Systematic uncertainties

Several sources of systematic uncertainty on $R_{\Lambda_c^+/D^0}$ are considered. For the signal extraction, three parametrizations of the CB functions are combined with the two background shapes. The systematic uncertainties are taken as the RMS of the results of all the fits for a given bin, considered as uncorrelated between the kinematic intervals. A similar strategy is employed for the prompt fraction estimation, where the Gaussian function is replaced by a Bukin function [57].

Four sources of systematic uncertainty are considered for the iterative method used to compute $\epsilon_{\rm rec\&sel}$ and $\epsilon_{\rm PID}$: (i) the uncertainty on the k factor; (ii) the choice of the binning used for the reference raw data distribution; (iii) the sensitivity to the initial reference data distribution; (iv) the uncertainty on the PID maps. The general strategy consists of performing the iterative procedure by varying individually each source of uncertainty within their uncertainties. For each source, $\epsilon_{\rm rec\&sel}$ and $\epsilon_{\rm PID}$ are computed by changing the configuration, and the RMS of all the variations are taken as the systematic uncertainties. For the first source, new results have been obtained on $R_{\Lambda_c^+/D^0}$ using 20 values of k, varied within uncertainties. The systematic uncertainty associated with the choice of the binning scheme (i.e second source) is evaluated by using a finer scheme than the nominal one. The sensitivity to the initial reference distributions (i.e third source) is tested by evaluating them using the *sPlot* technique instead of a fit of invariant-mass spectra. Finally, the uncertainty linked to the PID maps (i.e fourth source) is evaluated using a smearing technique to compute 20 PID maps where the efficiency in each bin is randomly varied within its statistical uncertainty.

Finally, the last sources of uncertainty considered are the statistical uncertainty coming from the size of the Monte Carlo sample ($\epsilon_{\rm tot}$ (stat.)) after the iterative procedure, and the statistical uncertainty on the acceptance.

All the systematic uncertainties are summarized in table 3. Each uncertainty category is treated as uncorrelated and is added in quadrature. Systematic uncertainty arising from the $\mathcal{B}$ ratio of $D^0 \to K^-\pi^+$ and $\Lambda_c^+ \to pK^-\pi^+$ decays, entering eq. (3.1), is also included in table 3. This contribution is fully correlated between different kinematic variable intervals.

5 Results

Results for the $R_{\Lambda_c^+/D^0}$ production ratio are given in table 4. The N_c variable is replaced by $\langle {\rm N_{part}} \rangle$ as shown in table 1. As can be seen in figure 3, the $p_{\rm T}$-integrated $R_{\Lambda_c^+/D^0}$ shows

JHEP06(2023)132

Source	N_c	p_{T} (GeV/c)	y
ϵ_{tot} (stat.)	5.1–7.1	4.1–5.1	4.1–7.1
Invariant-mass fit	1–5	1–5	1–5
f_{prompt}	1.8–8.1	1.4–10.2	3.4–4.6
ϵ_{acc}	<1	<1	<1
Iterative procedure	7–9	4–11	4–8
Total	9–12	8–14	8–10
Ratio of decay branching fractions	5.16	5.16	5.16

Table 3. Summary of the ranges of systematic uncertainties for the considered intervals of N_c, p_{T} and y for the $R_{\Lambda_c^+/D^0}$ ratio given in percentage.

p_{T} (GeV/c)	$R_{\Lambda_c^+/D^0}$
2–3	$0.188 \pm 0.095 \pm 0.025$
3–4	$0.389 \pm 0.072 \pm 0.029$
4–5	$0.349 \pm 0.052 \pm 0.040$
5–6	$0.272 \pm 0.049 \pm 0.036$
6–8	$0.235 \pm 0.035 \pm 0.032$
y	$R_{\Lambda_c^+/D^0}$
2.0–2.5	$0.288 \pm 0.044 \pm 0.029$
2.5–3.0	$0.292 \pm 0.048 \pm 0.028$
3.0–3.5	$0.246 \pm 0.056 \pm 0.020$
3.5–4.5	$0.120 \pm 0.067 \pm 0.011$
$\langle \mathrm{N_{part}} \rangle \pm \sigma_{\mathrm{part}}$	$R_{\Lambda_c^+/D^0}$
6.5 ± 2.5	$0.288 \pm 0.029 \pm 0.034$
12.4 ± 4.4	$0.253 \pm 0.029 \pm 0.022$
26.6 ± 7.5	$0.227 \pm 0.071 \pm 0.024$

Table 4. Results for the prompt $R_{\Lambda_c^+/D^0}$ production ratio, where the first uncertainties are statistical and the second systematic. A fully correlated systematic uncertainty of 5.16%, due to the limited knowledge of the external decay branching fractions, affects all the intervals.

no dependence on $\langle \mathrm{N_{part}} \rangle$, within uncertainties, with a mean value $\langle R_{\Lambda_c^+/D^0} \rangle \sim 0.27$. In figure 4, the p_{T} and $|y^*|$ dependent $R_{\Lambda_c^+/D^0}$ results are compared to those from pPb data at $\sqrt{s_{\mathrm{NN}}} = 5.02$ TeV [29], showing a good agreement between the measurements. Here $|y^*|$ is defined as the absolute value of rapidity in the center-of-mass system (y^*). Due to the beam boost, the pPb (proton beam towards LHCb) and Pbp (lead beam towards LHCb) data were recorded at forward ($1.5 < y^* < 4.0$) and backward ($-4.5 < y^* < -2.5$) rapidity, the direction of the proton beam pointing toward the LHCb acceptance for positive y^* values. This observation is consistent with the fact that the two samples have relatively close center-of-mass energy, and similar $\langle \mathrm{N_{part}} \rangle$ values ($\langle \mathrm{N_{part}} \rangle \sim 7.9$ in pPb collisions at $\sqrt{s_{\mathrm{NN}}} = 5.02$ TeV as measured by ALICE [58]). The same measurements of $R_{\Lambda_c^+/D^0}$ versus p_{T} and y are compared to theoretical predictions in figure 5. Both dependencies are compared

JHEP06(2023)132

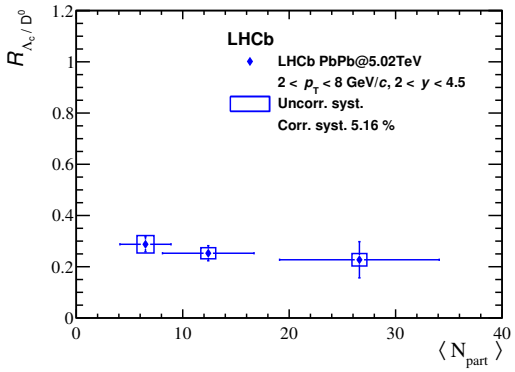

Figure 3. Prompt $R_{\Lambda_c^+/D^0}$ production ratios as a function of $\langle \mathrm{N_{part}} \rangle$. The error bars along the y-axis (x-axis) represent the statistical uncertainties (RMS of the $\langle \mathrm{N_{part}} \rangle$ value), the boxes around the points the uncorrelated systematic uncertainties.

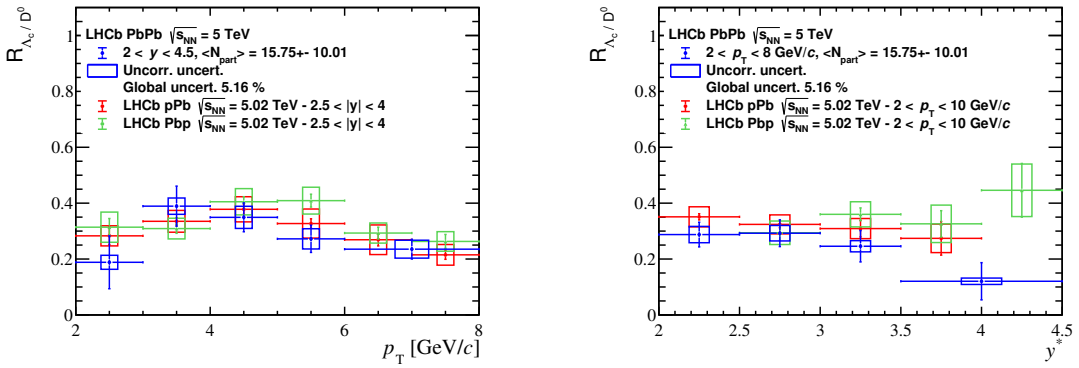

Figure 4. Prompt $R_{\Lambda_c^+/D^0}$ production ratios as a function of (left) p_{T} and (right) rapidity, with y^* being the rapidity in the centre-of-mass system for the pPb and Pbp results.The error bars represent the statistical uncertainties, the boxes around the points the uncorrelated systematic uncertainties. Results are compared to the same measurement in pPb and Pbp collisions at $\sqrt{s_{\mathrm{NN}}} = 5.02\,\mathrm{TeV}$ by the LHCb experiment [43].

to predictions from PYTHIA 8 [18] in pp collisions at $\sqrt{s} = 5.02$ TeV using the beyond-the-leading-color contributions. For these predictions, a special tuning is used to increase the Λ_c^+ color-reconnection mechanism at the expense of D mesons (see appendix A). In addition, the CR mechanism is also allowed. A good description of the p_{T} trend is found between theory and data for $p_{\mathrm{T}} > 3\,\mathrm{GeV}/c$, while tensions are observed at $p_{\mathrm{T}} < 3\,\mathrm{GeV}/c$. The model predicts a constant trend with rapidity and overshoots systematically the data by up to three standard deviations. The p_{T} dependence is also compared to predictions from the SHM [27] for which an augmented set of excited charm-baryon states decaying into Λ_c^+ is considered, and where fragmentation functions are used to compute the charm-hadron p_{T} spectra. The uncertainty band encompasses the uncertainty from varying the branching fractions from 50% to 100%. According to this model, these additional states could explain the large $R_{\Lambda_c^+/D^0}$ observed by the ALICE experiment at mid-rapidity in pp and pPb collisions at $\sqrt{s_{\mathrm{NN}}} = 5.02\,\mathrm{TeV}$ [14, 15]. These predictions are systematically

JHEP06(2023)132

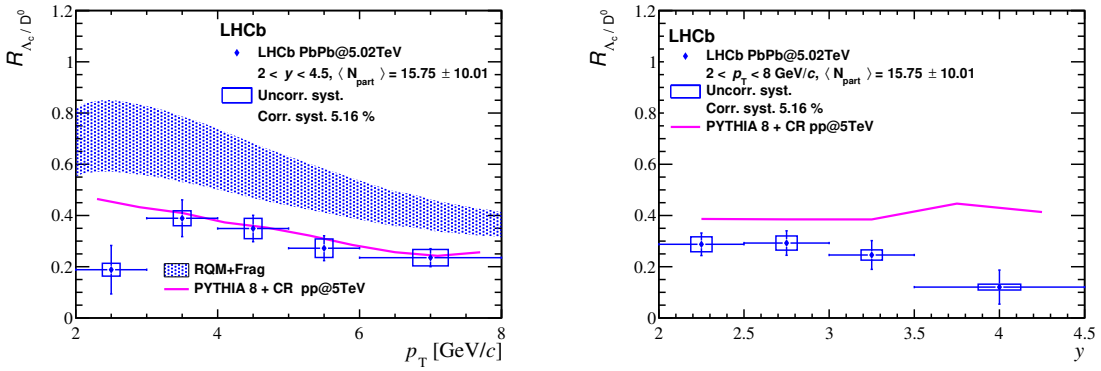

Figure 5. Prompt $R_{\Lambda_c^+/D^0}$ production ratios as a function of (left) p_{T} and (right) rapidity. The error bars represent the statistical uncertainties, the boxes around the points the uncorrelated systematic uncertainties. Results are compared to PYTHIA 8 [18] in pp collisions at $\sqrt{s} = 13\,\mathrm{TeV}$ (magenta band) and predictions from a Statical Hadronization Model [27] (blue band).

higher than the LHCb data versus p_{T}. Finally, plots comparing the present results to recent ALICE and STAR data can be found in appendix B.

6 Conclusions

This paper reports the first measurements of the $R_{\Lambda_c^+/D^0}$ production cross-section ratio in peripheral PbPb collisions at $\sqrt{s_{\mathrm{NN}}} = 5.02\,\mathrm{TeV}$ by the LHCb experiment. The $R_{\Lambda_c^+/D^0}$ shows no significant dependence on either rapidity or $\langle \mathrm{N_{part}} \rangle$ in peripheral collisions within uncertainties and has a mean value of $\langle R_{\Lambda_c^+/D^0} \rangle \sim 0.27$. However, the ratio tends to decrease at lower p_{T}. More data are needed to confirm the results. Results are consistent with previous LHCb measurements in pPb collisions at $\sqrt{s_{\mathrm{NN}}} = 5.02\,\mathrm{TeV}$ [43]. Compared to theory predictions, the results are compatible within one standard deviation with the PYTHIA 8 predictions in pp collisions at $\sqrt{s} = 5.02\,\mathrm{TeV}$, including the CR mechanism at next-to-leading color approximation, except at low p_{T}. In contrast, a systematic discrepancy versus p_{T} is observed with the SHM model predictions with an extended set of baryon states. These new experimental results point toward a strong dependence of $R_{\Lambda_c^+/D^0}$ on rapidity when compared to ALICE measurements at mid-rapidity in pp and pPb collisions [15], which could help to constrain theory predictions in this particular phase-space region.

Acknowledgments

We express our gratitude to our colleagues in the CERN accelerator departments for the excellent performance of the LHC. We thank the technical and administrative staff at the LHCb institutes. We acknowledge support from CERN and from the national agencies: CAPES, CNPq, FAPERJ and FINEP (Brazil); MOST and NSFC (China); CNRS/IN2P3 (France); BMBF, DFG and MPG (Germany); INFN (Italy); NWO (Netherlands); MNiSW and NCN (Poland); MEN/IFA (Romania); MICINN (Spain); SNSF and SER (Switzer-

JHEP06(2023)132

land); NASU (Ukraine); STFC (United Kingdom); DOE NP and NSF (USA). We acknowledge the computing resources that are provided by CERN, IN2P3 (France), KIT and DESY (Germany), INFN (Italy), SURF (Netherlands), PIC (Spain), GridPP (United Kingdom), CSCS (Switzerland), IFIN-HH (Romania), CBPF (Brazil), Polish WLCG (Poland) and NERSC (USA). We are indebted to the communities behind the multiple open-source software packages on which we depend. Individual groups or members have received support from ARC and ARDC (Australia); Minciencias (Colombia); AvH Foundation (Germany); EPLANET, Marie Skłodowska-Curie Actions and ERC (European Union); A*MIDEX, ANR, IPhU and Labex P2IO, and Région Auvergne-Rhône-Alpes (France); Key Research Program of Frontier Sciences of CAS, CAS PIFI, CAS CCEPP, Fundamental Research Funds for the Central Universities, and Sci. & Tech. Program of Guangzhou (China); GVA, XuntaGal, GENCAT and Prog. Atracción Talento, CM (Spain); SRC (Sweden); the Leverhulme Trust, the Royal Society and UKRI (United Kingdom).

A PYTHIA 8 tuning

The parameters of the Pythia tuning used to produce the results shown in figure 5 are reported in table 5.

Parameter	Value
SoftQCD:all	on
StringFlav:probQQ1toQQ0join	0.0275,0.0275,0.0275,0.0275
StringFlav:probQQtoQ	0.0780000
StringFlav:ProbStoUD	0.2
StringZ:aLund	0.36
StringZ:bLund	0.56
StringFlav:mesonCvector	1.35
ColourReconnection:mode	1
BeamRemnants:remnantMode	1
ColourReconnection:allowDoubleJunRem	off
MultipartonInteractions:pT0Ref	2.15
PartonVertex:ProtonRadius	0.7
PartonVertex:setVertex	on
Ropewalk:beta	0.1
Ropewalk:deltat	0.05
Ropewalk:doFlavour	on
Ropewalk:doShoving	on
Ropewalk:gAmplitude	0.0
Ropewalk:RopeHadronization	on
Ropewalk:tShove	0.1

Table 5. PYTHIA 8 tuning used for the theory predictions.

JHEP06(2023)132

B Comparison to other experiments

In this appendix, the results from this paper are compared to measurements from other experiments.

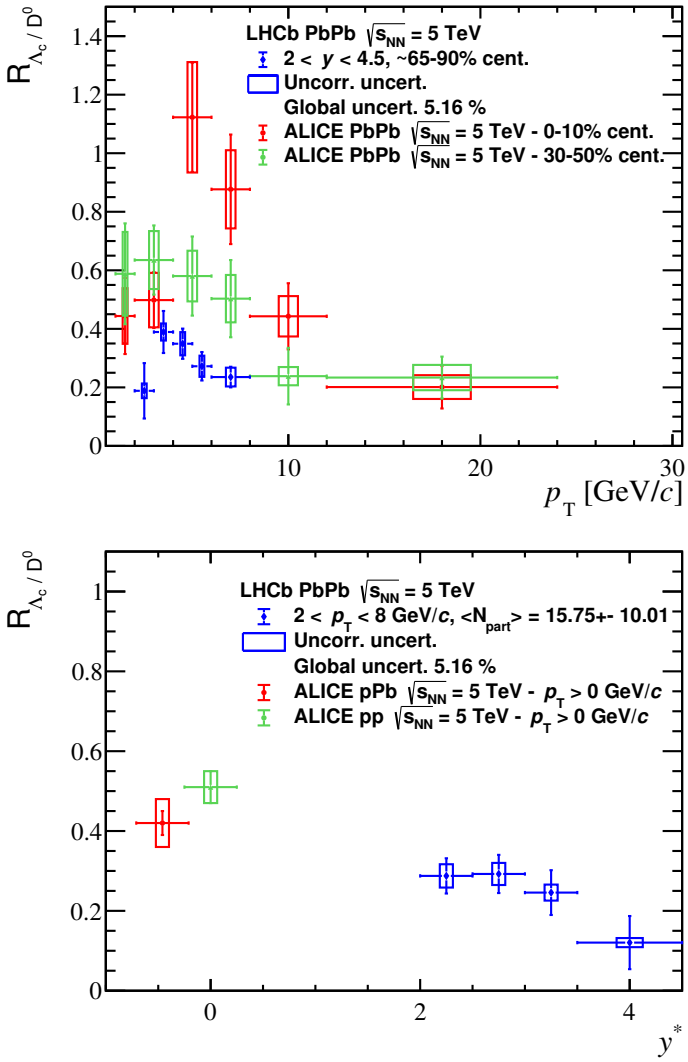

Figure 6. Prompt $R_{\Lambda_c^+/D^0}$ production ratios as a function of (top) p_{T} and (bottom) rapidity in the centre-of-mass system. The error bars represent the statistical uncertainties and the boxes around the points the uncorrelated systematic uncertainties. On the top panel, results are compared to the ALICE measurements in PbPb collisions at $\sqrt{s_{\mathrm{NN}}} = 5.02\,\mathrm{TeV}$ [16] measured in (red) 0-10% and (green) 30-50% centrality range. On the bottom panel, results are compared to the ALICE measurements (green) in pp and (red) pPb collisions at $\sqrt{s_{\mathrm{NN}}} = 5.02\,\mathrm{TeV}$ [15].

JHEP06(2023)132

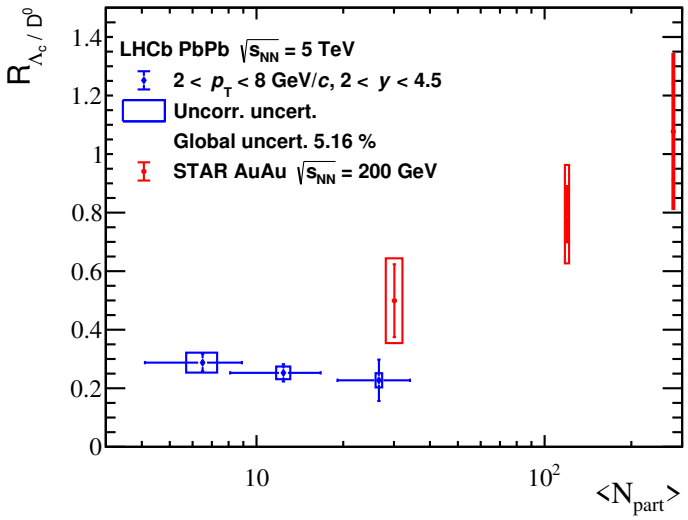

Figure 7. Prompt $R_{\Lambda_c^+/D^0}$ production ratios as a function of $\langle \mathrm{N_{part}} \rangle$. The error bars represent the statistical uncertainties, and the boxes around the points are the uncorrelated systematic uncertainties. Results are compared to the STAR measurements in Au-Au collisions at $\sqrt{s_{\mathrm{NN}}} = 200\,\mathrm{GeV}$ [21].

References

[1] P. Braun-Munzinger, V. Koch, T. Schäfer and J. Stachel, *Properties of hot and dense matter from relativistic heavy ion collisions*, *Phys. Rept.* **621** (2016) 76 [arXiv:1510.00442] [INSPIRE].

[2] HotQCD collaboration, *Equation of state in* $(2+1)$*-flavor QCD*, *Phys. Rev. D* **90** (2014) 094503 [arXiv:1407.6387] [INSPIRE].

[3] P.B. Gossiaux, *Open Heavy Flavors in Nuclear Collisions: Theory Overview*, *Nucl. Phys. A* **982** (2019) 113 [arXiv:1901.01606] [INSPIRE].

[4] A. Andronic et al., *Heavy-flavour and quarkonium production in the LHC era: from proton-proton to heavy-ion collisions*, *Eur. Phys. J. C* **76** (2016) 107 [arXiv:1506.03981] [INSPIRE].

[5] F. Prino and R. Rapp, *Open Heavy Flavor in QCD Matter and in Nuclear Collisions*, *J. Phys. G* **43** (2016) 093002 [arXiv:1603.00529] [INSPIRE].

[6] X. Dong, Y.-J. Lee and R. Rapp, *Open Heavy-Flavor Production in Heavy-Ion Collisions*, *Ann. Rev. Nucl. Part. Sci.* **69** (2019) 417 [arXiv:1903.07709] [INSPIRE].

[7] CLEO collaboration, *Charm meson spectra in* e^+e^- *annihilation at 10.5 GeV center of mass energy*, *Phys. Rev. D* **70** (2004) 112001 [hep-ex/0402040] [INSPIRE].

JHEP06(2023)132

[8] Belle collaboration, *Charm hadrons from fragmentation and B decays in e^+e^- annihilation at $\sqrt{s} = 10.6\,GeV$*, *Phys. Rev. D* **73** (2006) 032002 [hep-ex/0506068] [INSPIRE].

[9] BaBar collaboration, *Measurement of D_s^+ and D_s^{*+} production in B meson decays and from continuum e^+e^- annihilation at $\sqrt{s} = 10.6$ GeV*, *Phys. Rev. D* **65** (2002) 091104 [hep-ex/0201041] [INSPIRE].

[10] LHCb collaboration, *Prompt charm production in pp collisions at $\sqrt{s} = 7$ TeV*, *Nucl. Phys. B* **871** (2013) 1 [arXiv:1302.2864] [INSPIRE].

[11] LHCb collaboration, *Measurements of prompt charm production cross-sections in pp collisions at $\sqrt{s} = 13$ TeV*, *JHEP* **03** (2016) 159 [arXiv:1510.01707] [*Erratum ibid.* **09** (2016) 013] [INSPIRE].

[12] LHCb collaboration, *Measurements of prompt charm production cross-sections in pp collisions at $\sqrt{s} = 5$ TeV*, *JHEP* **06** (2017) 147 [arXiv:1610.02230] [INSPIRE].

[13] ALICE collaboration, *Λ_c^+ production in pp collisions at $\sqrt{s} = 7$ TeV and in p-Pb collisions at $\sqrt{s_{\rm NN}} = 5.02$ TeV*, *JHEP* **04** (2018) 108 [arXiv:1712.09581] [INSPIRE].

[14] ALICE collaboration, *Λ_c^+ production in Pb-Pb collisions at $\sqrt{s_{\rm NN}} = 5.02$ TeV*, *Phys. Lett. B* **793** (2019) 212 [arXiv:1809.10922] [INSPIRE].

[15] ALICE collaboration, *Λ_c^+ production in pp and in p-Pb collisions at $\sqrt{s_{NN}} = 5.02$ TeV*, *Phys. Rev. C* **104** (2021) 054905 [arXiv:2011.06079] [INSPIRE].

[16] ALICE collaboration, *Constraining hadronization mechanisms with Λ_c^+/D^0 production ratios in Pb-Pb collisions at $\sqrt{s_{\rm NN}} = 5.02$ TeV*, *Phys. Lett. B* **839** (2023) 137796 [arXiv:2112.08156] [INSPIRE].

[17] T. Sjostrand, S. Mrenna and P.Z. Skands, *A brief Introduction to PYTHIA 8.1*, *Comput. Phys. Commun.* **178** (2008) 852 [arXiv:0710.3820] [INSPIRE].

[18] J.R. Christiansen and P.Z. Skands, *String formation beyond leading colour*, *JHEP* **08** (2015) 003 [arXiv:1505.01681] [INSPIRE].

[19] ALICE collaboration, *Observation of a multiplicity dependence in the $p_{\rm T}$-differential charm baryon-to-meson ratios in proton-proton collisions at $\sqrt{s} = 13$ TeV*, *Phys. Lett. B* **829** (2022) 137065 [arXiv:2111.11948] [INSPIRE].

[20] CMS collaboration, *Production of Λ_c^+ baryons in proton-proton and lead-lead collisions at $\sqrt{s_{\rm NN}} = 5.02$ TeV*, *Phys. Lett. B* **803** (2020) 135328 [arXiv:1906.03322] [INSPIRE].

[21] STAR collaboration, *First measurement of Λ_c baryon production in Au+Au collisions at $\sqrt{s_{\rm NN}} = 200$ GeV*, *Phys. Rev. Lett.* **124** (2020) 172301 [arXiv:1910.14628] [INSPIRE].

[22] Y. Oh, C.M. Ko, S.H. Lee and S. Yasui, *Heavy baryon/meson ratios in relativistic heavy ion collisions*, *Phys. Rev. C* **79** (2009) 044905 [arXiv:0901.1382] [INSPIRE].

[23] S. Plumari, V. Minissale, S.K. Das, G. Coci and V. Greco, *Charmed hadrons from coalescence plus fragmentation in relativistic nucleus-nucleus collisions at RHIC and LHC*, *Eur. Phys. J. C* **78** (2018) 348 [arXiv:1712.00730] [INSPIRE].

[24] A. Beraudo, A. De Pace, M. Monteno, M. Nardi and F. Prino, *In-medium hadronization of heavy quarks and its effect on charmed meson and baryon distributions in heavy-ion collisions*, *Eur. Phys. J. C* **82** (2022) 607 [arXiv:2202.08732] [INSPIRE].

[25] S. Cho, K.-J. Sun, C.M. Ko, S.H. Lee and Y. Oh, *Charmed hadron production in an improved quark coalescence model*, *Phys. Rev. C* **101** (2020) 024909 [arXiv:1905.09774] [INSPIRE].

JHEP06(2023)132

[26] J. Zhao, S. Shi, N. Xu and P. Zhuang, *Sequential Coalescence with Charm Conservation in High Energy Nuclear Collisions*, arXiv:1805.10858 [INSPIRE].

[27] M. He and R. Rapp, *Charm-Baryon Production in Proton-Proton Collisions*, *Phys. Lett. B* **795** (2019) 117 [arXiv:1902.08889] [INSPIRE].

[28] M. He and R. Rapp, *Hadronization and charm-hadron ratios in heavy-ion collisions*, *Phys. Rev. Lett.* **124** (2020) 042301 [arXiv:1905.09216] [INSPIRE].

[29] LHCb collaboration, *Prompt Λ_c^+ production in* pPb *collisions at* $\sqrt{s_{NN}} = 5.02$ *TeV*, *JHEP* **02** (2019) 102 [arXiv:1809.01404] [INSPIRE].

[30] K.J. Eskola, H. Paukkunen and C.A. Salgado, *EPS09: A New Generation of NLO and LO Nuclear Parton Distribution Functions*, *JHEP* **04** (2009) 065 [arXiv:0902.4154] [INSPIRE].

[31] K. Kovarik et al., *nCTEQ15 — Global analysis of nuclear parton distributions with uncertainties in the CTEQ framework*, *Phys. Rev. D* **93** (2016) 085037 [arXiv:1509.00792] [INSPIRE].

[32] J.-P. Lansberg and H.-S. Shao, *Towards an automated tool to evaluate the impact of the nuclear modification of the gluon density on quarkonium, D and B meson production in proton-nucleus collisions*, *Eur. Phys. J. C* **77** (2017) 1 [arXiv:1610.05382] [INSPIRE].

[33] H.-S. Shao, *HELAC-Onia 2.0: an upgraded matrix-element and event generator for heavy quarkonium physics*, *Comput. Phys. Commun.* **198** (2016) 238 [arXiv:1507.03435] [INSPIRE].

[34] H.-S. Shao, *HELAC-Onia: An automatic matrix element generator for heavy quarkonium physics*, *Comput. Phys. Commun.* **184** (2013) 2562 [arXiv:1212.5293] [INSPIRE].

[35] LHCb collaboration, *The LHCb detector at the LHC*, 2008 *JINST* **3** S08005 [INSPIRE].

[36] LHCb collaboration, *LHCb detector performance*, *Int. J. Mod. Phys. A* **30** (2015) 1530022 [arXiv:1412.6352] [INSPIRE].

[37] R. Aaij et al., *Performance of the LHCb Vertex Locator*, 2014 *JINST* **9** P09007 [arXiv:1405.7808] [INSPIRE].

[38] LHCb Outer Tracker Group collaboration, *Improved performance of the LHCb Outer Tracker in LHC Run 2*, 2017 *JINST* **12** P11016 [arXiv:1708.00819] [INSPIRE].

[39] LHCb RICH Group collaboration, *Performance of the LHCb RICH detector at the LHC*, *Eur. Phys. J. C* **73** (2013) 2431 [arXiv:1211.6759] [INSPIRE].

[40] A.A. Alves, Jr. et al., *Performance of the LHCb muon system*, 2013 *JINST* **8** P02022 [arXiv:1211.1346] [INSPIRE].

[41] R. Aaij et al., *The LHCb trigger and its performance in 2011*, 2013 *JINST* **8** P04022 [arXiv:1211.3055] [INSPIRE].

[42] LHCb collaboration, *Precision luminosity measurements at LHCb*, 2014 *JINST* **9** P12005 [arXiv:1410.0149] [INSPIRE].

[43] LHCb collaboration, *Prompt Λ_c^+ production in* pPb *collisions at* $\sqrt{s_{NN}} = 5.02$ *TeV*, *JHEP* **02** (2019) 102 [arXiv:1809.01404] [INSPIRE].

[44] S. Porteboeuf, T. Pierog and K. Werner, *Producing Hard Processes Regarding the Complete Event: The EPOS Event Generator*, in *45th Rencontres de Moriond on QCD and High Energy Interactions*, La Thuile, Italy, (2010), pg. 135 [arXiv:1006.2967] [INSPIRE].

JHEP06(2023)132

[45] T. Pierog, I. Karpenko, J.M. Katzy, E. Yatsenko and K. Werner, *EPOS LHC: Test of collective hadronization with data measured at the CERN Large Hadron Collider*, *Phys. Rev. C* **92** (2015) 034906 [arXiv:1306.0121] [INSPIRE].

[46] D.J. Lange, *The EvtGen particle decay simulation package*, *Nucl. Instrum. Meth. A* **462** (2001) 152 [INSPIRE].

[47] P. Golonka and Z. Was, *PHOTOS Monte Carlo: A Precision tool for QED corrections in Z and W decays*, *Eur. Phys. J. C* **45** (2006) 97 [hep-ph/0506026] [INSPIRE].

[48] GEANT4 collaboration, *GEANT4 — a simulation toolkit*, *Nucl. Instrum. Meth. A* **506** (2003) 250 [INSPIRE].

[49] J. Allison et al., *Geant4 developments and applications*, *IEEE Trans. Nucl. Sci.* **53** (2006) 270 [INSPIRE].

[50] LHCb collaboration, *The LHCb simulation application, Gauss: Design, evolution and experience*, *J. Phys. Conf. Ser.* **331** (2011) 032023 [INSPIRE].

[51] Particle Data Group collaboration, *Review of Particle Physics*, *PTEP* **2020** (2020) 083C01 [INSPIRE].

[52] C. Loizides, J. Nagle and P. Steinberg, *Improved version of the PHOBOS Glauber Monte Carlo*, *SoftwareX* **1-2** (2015) 13 [arXiv:1408.2549] [INSPIRE].

[53] LHCb collaboration, *Centrality determination in heavy-ion collisions with the LHCb detector*, 2022 *JINST* **17** P05009 [arXiv:2111.01607] [INSPIRE].

[54] T. Skwarnicki, *A study of the radiative CASCADE transitions between the Upsilon-Prime and Upsilon resonances*, Ph.D. Thesis, Institute of Nuclear Physics, Krakow, Poland (1986) [INSPIRE].

[55] M. Pivk and F.R. Le Diberder, *SPlot: A Statistical tool to unfold data distributions*, *Nucl. Instrum. Meth. A* **555** (2005) 356 [physics/0402083] [INSPIRE].

[56] ATLAS collaboration, *Prospect for a search for direct stau production in events with at least two hadronic taus and missing transverse momentum at theHigh Luminosity LHC with the ATLAS Detector*, ATL-PHYS-PUB-2016-021 (2016).

[57] A.D. Bukin, *Fitting function for asymmetric peaks*, arXiv:0711.4449 [INSPIRE].

[58] ALICE collaboration, *Centrality dependence of particle production in p-Pb collisions at* $\sqrt{s_{\rm NN}} = 5.02$ *TeV*, *Phys. Rev. C* **91** (2015) 064905 [arXiv:1412.6828] [INSPIRE].

JHEP06(2023)132

The LHCb collaboration

R. Aaij[32], A.S.W. Abdelmotteleb[50], C. Abellan Beteta[44], F. Abudinén[50], T. Ackernley[54], B. Adeva[40], M. Adinolfi[48], H. Afsharnia[9], C. Agapopoulou[13], C.A. Aidala[76], S. Aiola[25], Z. Ajaltouni[9], S. Akar[59], K. Akiba[32], J. Albrecht[15], F. Alessio[42], M. Alexander[53], A. Alfonso Albero[39], Z. Aliouche[56], P. Alvarez Cartelle[49], S. Amato[2], J.L. Amey[48], Y. Amhis[11,42], L. An[42], L. Anderlini[22], M. Andersson[44], A. Andreianov[38], M. Andreotti[21], D. Andreou[62], D. Ao[6], F. Archilli[17], A. Artamonov[38], M. Artuso[62], E. Aslanides[10], M. Atzeni[44], B. Audurier[12], S. Bachmann[17], M. Bachmayer[43], J.J. Back[50], A. Bailly-reyre[13], P. Baladron Rodriguez[40], V. Balagura[12], W. Baldini[21], J. Baptista de Souza Leite[1], M. Barbetti[22,j], R.J. Barlow[56], S. Barsuk[11], W. Barter[55], M. Bartolini[49], F. Baryshnikov[38], J.M. Basels[14], G. Bassi[29,q], B. Batsukh[4], A. Battig[15], A. Bay[43], A. Beck[50], M. Becker[15], F. Bedeschi[29], I.B. Bediaga[1], A. Beiter[62], V. Belavin[38], S. Belin[40], V. Bellee[44], K. Belous[38], I. Belov[38], I. Belyaev[38], G. Bencivenni[23], E. Ben-Haim[13], A. Berezhnoy[38], R. Bernet[44], D. Berninghoff[17], H.C. Bernstein[62], C. Bertella[56], A. Bertolin[28], C. Betancourt[44], F. Betti[42], Ia. Bezshyiko[44], S. Bhasin[48], J. Bhom[35], L. Bian[67], M.S. Bieker[15], N.V. Biesuz[21], S. Bifani[47], P. Billoir[13], A. Biolchini[32], M. Birch[55], F.C.R. Bishop[49], A. Bitadze[56], A. Bizzeti, M.P. Blago[49], T. Blake[50], F. Blanc[43], S. Blusk[62], D. Bobulska[53], J.A. Boelhauve[15], O. Boente Garcia[40], T. Boettcher[59], A. Boldyrev[38], N. Bondar[38,42], S. Borghi[56], M. Borsato[17], J.T. Borsuk[35], S.A. Bouchiba[43], T.J.V. Bowcock[54,42], A. Boyer[42], C. Bozzi[21], M.J. Bradley[55], S. Braun[60], A. Brea Rodriguez[40], J. Brodzicka[35], A. Brossa Gonzalo[50], D. Brundu[27], A. Buonaura[44], L. Buonincontri[28], A.T. Burke[56], C. Burr[42], A. Bursche[66], A. Butkevich[38], J.S. Butter[32], J. Buytaert[42], W. Byczynski[42], S. Cadeddu[27], H. Cai[67], R. Calabrese[21,i], L. Calefice[15,13], S. Cali[23], R. Calladine[47], M. Calvi[26,m], M. Calvo Gomez[74], P. Camargo Magalhaes[48], P. Campana[23], D.H. Campora Perez[73], A.F. Campoverde Quezada[6], S. Capelli[26,m], L. Capriotti[20,g], A. Carbone[20,g], G. Carboni[31], R. Cardinale[24,k], A. Cardini[27], I. Carli[4], P. Carniti[26,m], L. Carus[14], A. Casais Vidal[40], R. Caspary[17], G. Casse[54], M. Cattaneo[42], G. Cavallero[42], V. Cavallini[21,i], S. Celani[43], J. Cerasoli[10], D. Cervenkov[57], A.J. Chadwick[54], M.G. Chapman[48], M. Charles[13], Ph. Charpentier[42], C.A. Chavez Barajas[54], M. Chefdeville[8], C. Chen[3], S. Chen[4], A. Chernov[35], S. Chernyshenko[46], V. Chobanova[40], S. Cholak[43], M. Chrzaszcz[35], A. Chubykin[38], V. Chulikov[38], P. Ciambrone[23], M.F. Cicala[50], X. Cid Vidal[40], G. Ciezarek[42], G. Ciullo[i,21], P.E.L. Clarke[52], M. Clemencic[42], H.V. Cliff[49], J. Closier[42], J.L. Cobbledick[56], V. Coco[42], J.A.B. Coelho[11], J. Cogan[10], E. Cogneras[9], L. Cojocariu[37], P. Collins[42], T. Colombo[42], L. Congedo[19,f], A. Contu[27], N. Cooke[47], G. Coombs[53], I. Corredoira [40], G. Corti[42], B. Couturier[42], D.C. Craik[58], J. Crkovská[61], M. Cruz Torres[1,e], R. Currie[52], C.L. Da Silva[61], S. Dadabaev[38], L. Dai[65], E. Dall'Occo[15], J. Dalseno[40], C. D'Ambrosio[42], A. Danilina[38], P. d'Argent[15], J.E. Davies[56], A. Davis[56], O. De Aguiar Francisco[56], J. de Boer[42], K. De Bruyn[72], S. De Capua[56], M. De Cian[43], U. De Freitas Carneiro Da Graca[1], E. De Lucia[23], J.M. De Miranda[1], L. De Paula[2], M. De Serio[19,f], D. De Simone[44],

JHEP06(2023)132

P. De Simone[23], F. De Vellis[15], J.A. de Vries[73], C.T. Dean[61], F. Debernardis[19,f], D. Decamp[8], V. Dedu[10], L. Del Buono[13], B. Delaney[49], H.-P. Dembinski[15], V. Denysenko[44], O. Deschamps[9], F. Dettori[27,h], B. Dey[70], A. Di Cicco[23], P. Di Nezza[23], S. Didenko[38], L. Dieste Maronas[40], S. Ding[62], V. Dobishuk[46], A. Dolmatov[38], C. Dong[3], A.M. Donohoe[18], F. Dordei[27], A.C. dos Reis[1], L. Douglas[53], A.G. Downes[8], M.W. Dudek[35], L. Dufour[42], V. Duk[71], P. Durante[42], J.M. Durham[61], D. Dutta[56], A. Dziurda[35], A. Dzyuba[38], S. Easo[51], U. Egede[63], V. Egorychev[38], S. Eidelman[38,†], S. Eisenhardt[52], S. Ek-In[43], L. Eklund[75], S. Ely[62], A. Ene[37], E. Epple[61], S. Escher[14], J. Eschle[44], S. Esen[44], T. Evans[56], L.N. Falcao[1], Y. Fan[6], B. Fang[67], S. Farry[54], D. Fazzini[26,m], M. Feo[42], A.D. Fernez[60], F. Ferrari[20], L. Ferreira Lopes[43], F. Ferreira Rodrigues[2], S. Ferreres Sole[32], M. Ferrillo[44], M. Ferro-Luzzi[42], S. Filippov[38], R.A. Fini[19], M. Fiorini[21,i], M. Firlej[34], K.M. Fischer[57], D.S. Fitzgerald[76], C. Fitzpatrick[56], T. Fiutowski[34], F. Fleuret[12], M. Fontana[13], F. Fontanelli[24,k], R. Forty[42], D. Foulds-Holt[49], V. Franco Lima[54], M. Franco Sevilla[60], M. Frank[42], E. Franzoso[21,i], G. Frau[17], C. Frei[42], D.A. Friday[53], J. Fu[6], Q. Fuehring[15], E. Gabriel[32], G. Galati[19,f], A. Gallas Torreira[40], D. Galli[20,g], S. Gambetta[52,42], Y. Gan[3], M. Gandelman[2], P. Gandini[25], Y. Gao[5], M. Garau[27,h], L.M. Garcia Martin[50], P. Garcia Moreno[39], J. García Pardiñas[26,m], B. Garcia Plana[40], F.A. Garcia Rosales[12], L. Garrido[39], C. Gaspar[42], R.E. Geertsema[32], D. Gerick[17], L.L. Gerken[15], E. Gersabeck[56], M. Gersabeck[56], T. Gershon[50], L. Giambastiani[28], V. Gibson[49], H.K. Giemza[36], A.L. Gilman[57], M. Giovannetti[23,t], A. Gioventù[40], P. Gironella Gironell[39], C. Giugliano[21,i], K. Gizdov[52], E.L. Gkougkousis[42], V.V. Gligorov[13,42], C. Göbel[64], E. Golobardes[74], D. Golubkov[38], A. Golutvin[55,38], A. Gomes[1,a], S. Gomez Fernandez[39], F. Goncalves Abrantes[57], M. Goncerz[35], G. Gong[3], I.V. Gorelov[38], C. Gotti[26], J.P. Grabowski[17], T. Grammatico[13], L.A. Granado Cardoso[42], E. Graugés[39], E. Graverini[43], G. Graziani[], A. T. Grecu[37], L.M. Greeven[32], N.A. Grieser[4], L. Grillo[53], S. Gromov[38], B.R. Gruberg Cazon[57], C. Gu[3], M. Guarise[21,i], M. Guittiere[11], P. A. Günther[17], E. Gushchin[38], A. Guth[14], Y. Guz[38], T. Gys[42], T. Hadavizadeh[63], G. Haefeli[43], C. Haen[42], J. Haimberger[42], S.C. Haines[49], T. Halewood-leagas[54], M.M. Halvorsen[42], P.M. Hamilton[60], J. Hammerich[54], Q. Han[7], X. Han[17], E.B. Hansen[56], S. Hansmann-Menzemer[17,42], L. Hao[6], N. Harnew[57], T. Harrison[54], C. Hasse[42], M. Hatch[42], J. He[6,c], K. Heijhoff[32], K. Heinicke[15], R.D.L. Henderson[63,50], A.M. Hennequin[58], K. Hennessy[54], L. Henry[42], J. Heuel[14], A. Hicheur[2], D. Hill[43], M. Hilton[56], S.E. Hollitt[15], R. Hou[7], Y. Hou[8], J. Hu[17], J. Hu[66], W. Hu[5], X. Hu[3], W. Huang[6], X. Huang[67], W. Hulsbergen[32], R.J. Hunter[50], M. Hushchyn[38], D. Hutchcroft[54], P. Ibis[15], M. Idzik[34], D. Ilin[38], P. Ilten[59], A. Inglessi[38], A. Iniukhin[38], A. Ishteev[38], K. Ivshin[38], R. Jacobsson[42], H. Jage[14], S. Jakobsen[42], E. Jans[32], B.K. Jashal[41], A. Jawahery[60], V. Jevtic[15], X. Jiang[4,6], M. John[57], D. Johnson[58], C.R. Jones[49], T.P. Jones[50], B. Jost[42], N. Jurik[42], S. Kandybei[45], Y. Kang[3], M. Karacson[42], D. Karpenkov[38], M. Karpov[38], J.W. Kautz[59], F. Keizer[42], D.M. Keller[62], M. Kenzie[50], T. Ketel[33], B. Khanji[15], A. Kharisova[38], S. Kholodenko[38], T. Kirn[14], V.S. Kirsebom[43], O. Kitouni[58], S. Klaver[33], N. Kleijne[29,q], K. Klimaszewski[36],

JHEP06(2023)132

M.R. Kmiec[36], S. Koliiev[46], A. Kondybayeva[38], A. Konoplyannikov[38], P. Kopciewicz[34], R. Kopecna[17], P. Koppenburg[32], M. Korolev[38], I. Kostiuk[32,46], O. Kot[46], S. Kotriakhova, A. Kozachuk[38], P. Kravchenko[38], L. Kravchuk[38], R.D. Krawczyk[42], M. Kreps[50], S. Kretzschmar[14], P. Krokovny[38], W. Krupa[34], W. Krzemien[36], J. Kubat[17], W. Kucewicz[35,34], M. Kucharczyk[35], V. Kudryavtsev[38], H.S. Kuindersma[32], G.J. Kunde[61], D. Lacarrere[42], G. Lafferty[56], A. Lai[27], A. Lampis[27,h], D. Lancierini[44], J.J. Lane[56], R. Lane[48], G. Lanfranchi[23], C. Langenbruch[14], J. Langer[15], O. Lantwin[38], T. Latham[50], F. Lazzari[29,u], M. Lazzaroni[25,l], R. Le Gac[10], S.H. Lee[76], R. Lefèvre[9], A. Leflat[38], S. Legotin[38], P. Lenisa[i,21], O. Leroy[10], T. Lesiak[35], B. Leverington[17], H. Li[66], K. Li[7], P. Li[17], S. Li[7], Y. Li[4], Z. Li[62], X. Liang[62], C. Lin[6], T. Lin[55], R. Lindner[42], V. Lisovskyi[15], R. Litvinov[27,h], G. Liu[66], H. Liu[6], Q. Liu[6], S. Liu[4,6], A. Lobo Salvia[39], A. Loi[27], R. Lollini[71], J. Lomba Castro[40], I. Longstaff[53], J.H. Lopes[2], S. López Soliño[40], G.H. Lovell[49], Y. Lu[4,b], C. Lucarelli[22,j], D. Lucchesi[28,o], S. Luchuk[38], M. Lucio Martinez[32], V. Lukashenko[32,46], Y. Luo[3], A. Lupato[56], E. Luppi[21,i], A. Lusiani[29,q], K. Lynch[18], X.-R. Lyu[6], L. Ma[4], R. Ma[6], S. Maccolini[20], F. Machefert[11], F. Maciuc[37], V. Macko[43], P. Mackowiak[15], S. Maddrell-Mander[48], L.R. Madhan Mohan[48], A. Maevskiy[38], D. Maisuzenko[38], M.W. Majewski[34], J.J. Malczewski[35], S. Malde[57], B. Malecki[35], A. Malinin[38], T. Maltsev[38], H. Malygina[17], G. Manca[27,h], G. Mancinelli[10], D. Manuzzi[20], C.A. Manzari[44], D. Marangotto[25,l], J.F. Marchand[8], U. Marconi[20], S. Mariani[22,j], C. Marin Benito[39], M. Marinangeli[43], J. Marks[17], A.M. Marshall[48], P.J. Marshall[54], G. Martelli[71,p], G. Martellotti[30], L. Martinazzoli[42,m], M. Martinelli[26,m], D. Martinez Santos[40], F. Martinez Vidal[41], A. Massafferri[1], M. Materok[14], R. Matev[42], A. Mathad[44], V. Matiunin[38], C. Matteuzzi[26], K.R. Mattioli[76], A. Mauri[32], E. Maurice[12], J. Mauricio[39], M. Mazurek[42], M. McCann[55], L. Mcconnell[18], T.H. McGrath[56], N.T. McHugh[53], A. McNab[56], R. McNulty[18], J.V. Mead[54], B. Meadows[59], G. Meier[15], D. Melnychuk[36], S. Meloni[26,m], M. Merk[32,73], A. Merli[25,l], L. Meyer Garcia[2], M. Mikhasenko[69,d], D.A. Milanes[68], E. Millard[50], M. Milovanovic[42], M.-N. Minard[8,†], A. Minotti[26,m], S.E. Mitchell[52], B. Mitreska[56], D.S. Mitzel[15], A. Mödden[15], R.A. Mohammed[57], R.D. Moise[55], S. Mokhnenko[38], T. Mombächer[40], I.A. Monroy[68], S. Monteil[9], M. Morandin[28], G. Morello[23], M.J. Morello[29,q], J. Moron[34], A.B. Morris[69], A.G. Morris[50], R. Mountain[62], H. Mu[3], F. Muheim[52], M. Mulder[72], K. Müller[44], C.H. Murphy[57], D. Murray[56], R. Murta[55], P. Muzzetto[27,h], P. Naik[48], T. Nakada[43], R. Nandakumar[51], T. Nanut[42], I. Nasteva[2], M. Needham[52], N. Neri[25,l], S. Neubert[69], N. Neufeld[42], P. Neustroev[38], R. Newcombe[55], E.M. Niel[43], S. Nieswand[14], N. Nikitin[38], N.S. Nolte[58], C. Normand[8,h,27], C. Nunez[76], A. Oblakowska-Mucha[34], V. Obraztsov[38], T. Oeser[14], D.P. O'Hanlon[48], S. Okamura[21,i], R. Oldeman[27,h], F. Oliva[52], M.E. Olivares[62], C.J.G. Onderwater[72], R.H. O'Neil[52], J.M. Otalora Goicochea[2], T. Ovsiannikova[38], P. Owen[44], A. Oyanguren[41], O. Ozcelik[52], K.O. Padeken[69], B. Pagare[50], P.R. Pais[42], T. Pajero[57], A. Palano[19], M. Palutan[23], Y. Pan[56], G. Panshin[38], A. Papanestis[51], M. Pappagallo[19,f], L.L. Pappalardo[21,i], C. Pappenheimer[59], W. Parker[60], C. Parkes[56], B. Passalacqua[21,i], G. Passaleva[22], A. Pastore[19], M. Patel[55], C. Patrignani[20,g],

JHEP06(2023)132

C.J. Pawley[73], A. Pearce[42], A. Pellegrino[32], M. Pepe Altarelli[42], S. Perazzini[20], D. Pereima[38], A. Pereiro Castro[40], P. Perret[9], M. Petric[53], K. Petridis[48], A. Petrolini[24,k], A. Petrov[38], S. Petrucci[52], M. Petruzzo[25], H. Pham[62], A. Philippov[38], R. Piandani[6], L. Pica[29,q], M. Piccini[71], B. Pietrzyk[8], G. Pietrzyk[11], M. Pili[57], D. Pinci[30], F. Pisani[42], M. Pizzichemi[26,m,42], V. Placinta[37], J. Plews[47], M. Plo Casasus[40], F. Polci[13,42], M. Poli Lener[23], M. Poliakova[62], A. Poluektov[10], N. Polukhina[38], I. Polyakov[62], E. Polycarpo[2], S. Ponce[42], D. Popov[6,42], S. Popov[38], S. Poslavskii[38], K. Prasanth[35], L. Promberger[42], C. Prouve[40], V. Pugatch[46], V. Puill[11], G. Punzi[29,r], H.R. Qi[3], W. Qian[6], N. Qin[3], S. Qu[3], R. Quagliani[43], N.V. Raab[18], R.I. Rabadan Trejo[6], B. Rachwal[34], J.H. Rademacker[48], R. Rajagopalan[62], M. Rama[29], M. Ramos Pernas[50], M.S. Rangel[2], F. Ratnikov[38], G. Raven[33,42], M. Rebollo De Miguel[41], M. Reboud[8], F. Redi[42], F. Reiss[56], C. Remon Alepuz[41], Z. Ren[3], V. Renaudin[57], P.K. Resmi[10], R. Ribatti[29,q], A.M. Ricci[27], S. Ricciardi[51], K. Rinnert[54], P. Robbe[11], G. Robertson[52], A.B. Rodrigues[43], E. Rodrigues[54], J.A. Rodriguez Lopez[68], E. Rodriguez Rodriguez[40], A. Rollings[57], P. Roloff[42], V. Romanovskiy[38], M. Romero Lamas[40], A. Romero Vidal[40], J.D. Roth[76,†], M. Rotondo[23], M.S. Rudolph[62], T. Ruf[42], R.A. Ruiz Fernandez[40], J. Ruiz Vidal[41], A. Ryzhikov[38], J. Ryzka[34], J.J. Saborido Silva[40], N. Sagidova[38], N. Sahoo[47], B. Saitta[27,h], M. Salomoni[42], C. Sanchez Gras[32], I. Sanderswood[41], R. Santacesaria[30], C. Santamarina Rios[40], M. Santimaria[23], E. Santovetti[31,t], D. Saranin[38], G. Sarpis[14], M. Sarpis[69], A. Sarti[30], C. Satriano[30,s], A. Satta[31], M. Saur[15], D. Savrina[38], H. Sazak[9], L.G. Scantlebury Smead[57], A. Scarabotto[13], S. Schael[14], S. Scherl[54], M. Schiller[53], H. Schindler[42], M. Schmelling[16], B. Schmidt[42], S. Schmitt[14], O. Schneider[43], A. Schopper[42], M. Schubiger[32], S. Schulte[43], M.H. Schune[11], R. Schwemmer[42], B. Sciascia[23,42], A. Sciuccati[42], S. Sellam[40], A. Semennikov[38], M. Senghi Soares[33], A. Sergi[24,k], N. Serra[44], L. Sestini[28], A. Seuthe[15], Y. Shang[5], D.M. Shangase[76], M. Shapkin[38], I. Shchemerov[38], L. Shchutska[43], T. Shears[54], L. Shekhtman[38], Z. Shen[5], S. Sheng[4,6], V. Shevchenko[38], E.B. Shields[26,m], Y. Shimizu[11], E. Shmanin[38], J.D. Shupperd[62], B.G. Siddi[21,i], R. Silva Coutinho[44], G. Simi[28], S. Simone[19,f], M. Singla[63], N. Skidmore[56], R. Skuza[17], T. Skwarnicki[62], M.W. Slater[47], I. Slazyk[21,i], J.C. Smallwood[57], J.G. Smeaton[49], E. Smith[44], M. Smith[55], A. Snoch[32], L. Soares Lavra[9], M.D. Sokoloff[59], F.J.P. Soler[53], A. Solomin[38,48], A. Solovev[38], I. Solovyev[38], F.L. Souza De Almeida[2], B. Souza De Paula[2], B. Spaan[15,†], E. Spadaro Norella[25,l], E. Spiridenkov[38], P. Spradlin[53], V. Sriskaran[42], F. Stagni[42], M. Stahl[59], S. Stahl[42], S. Stanislaus[57], O. Steinkamp[44], O. Stenyakin[38], H. Stevens[15], S. Stone[62,†], D. Strekalina[38], F. Suljik[57], J. Sun[27], L. Sun[67], Y. Sun[60], P. Svihra[56], P.N. Swallow[47], K. Swientek[34], A. Szabelski[36], T. Szumlak[34], M. Szymanski[42], S. Taneja[56], A.R. Tanner[48], M.D. Tat[57], A. Terentev[38], F. Teubert[42], E. Thomas[42], D.J.D. Thompson[47], K.A. Thomson[54], H. Tilquin[55], V. Tisserand[9], S. T'Jampens[8], M. Tobin[4], L. Tomassetti[21,i], G. Tonani[25,l], X. Tong[5], D. Torres Machado[1], D.Y. Tou[3], E. Trifonova[38], S.M. Trilov[48], C. Trippl[43], G. Tuci[6], A. Tully[43], N. Tuning[32,42], A. Ukleja[36], D.J. Unverzagt[17], E. Ursov[38], A. Usachov[32], A. Ustyuzhanin[38], U. Uwer[17], A. Vagner[38], V. Vagnoni[20], A. Valassi[42], G. Valenti[20],

JHEP06(2023)132

N. Valls Canudas[74], M. van Beuzekom[32], M. Van Dijk[43], H. Van Hecke[61], E. van Herwijnen[38], M. van Veghel[72], R. Vazquez Gomez[39], P. Vazquez Regueiro[40], C. Vázquez Sierra[42], S. Vecchi[21], J.J. Velthuis[48], M. Veltri[22,v], A. Venkateswaran[62], M. Veronesi[32], M. Vesterinen[50], D. Vieira[59], M. Vieites Diaz[43], X. Vilasis-Cardona[74], E. Vilella Figueras[54], A. Villa[20], P. Vincent[13], F.C. Volle[11], D. vom Bruch[10], A. Vorobyev[38], V. Vorobyev[38], N. Voropaev[38], K. Vos[73], R. Waldi[17], J. Walsh[29], C. Wang[17], J. Wang[5], J. Wang[4], J. Wang[3], J. Wang[67], M. Wang[5], R. Wang[48], Y. Wang[7], Z. Wang[44], Z. Wang[3], Z. Wang[6], J.A. Ward[50,63], N.K. Watson[47], D. Websdale[55], C. Weisser[58], B.D.C. Westhenry[48], D.J. White[56], M. Whitehead[53], A.R. Wiederhold[50], D. Wiedner[15], G. Wilkinson[57], M.K. Wilkinson[59], I. Williams[49], M. Williams[58], M.R.J. Williams[52], F.F. Wilson[51], W. Wislicki[36], M. Witek[35], L. Witola[17], C.P. Wong[61], G. Wormser[11], S.A. Wotton[49], H. Wu[62], K. Wyllie[42], Z. Xiang[6], D. Xiao[7], Y. Xie[7], A. Xu[5], J. Xu[6], L. Xu[3], M. Xu[50], Q. Xu[6], Z. Xu[9], Z. Xu[6], D. Yang[3], S. Yang[6], Y. Yang[6], Z. Yang[5], Z. Yang[60], Y. Yao[62], L.E. Yeomans[54], H. Yin[7], J. Yu[65], X. Yuan[62], E. Zaffaroni[43], M. Zavertyaev[16], M. Zdybal[35], O. Zenaiev[42], M. Zeng[3], D. Zhang[7], L. Zhang[3], S. Zhang[65], S. Zhang[5], Y. Zhang[5], Y. Zhang[57], A. Zharkova[38], A. Zhelezov[17], Y. Zheng[6], T. Zhou[5], X. Zhou[6], Y. Zhou[6], V. Zhovkovska[11], X. Zhu[3], X. Zhu[7], Z. Zhu[6], V. Zhukov[14,38], Q. Zou[4,6], S. Zucchelli[20,g], D. Zuliani[28], G. Cynic's[56]

[1] *Centro Brasileiro de Pesquisas Físicas (CBPF), Rio de Janeiro, Brazil*
[2] *Universidade Federal do Rio de Janeiro (UFRJ), Rio de Janeiro, Brazil*
[3] *Center for High Energy Physics, Tsinghua University, Beijing, China*
[4] *Institute Of High Energy Physics (IHEP), Beijing, China*
[5] *School of Physics State Key Laboratory of Nuclear Physics and Technology, Peking University, Beijing, China*
[6] *University of Chinese Academy of Sciences, Beijing, China*
[7] *Institute of Particle Physics, Central China Normal University, Wuhan, Hubei, China*
[8] *Université Savoie Mont Blanc, CNRS, IN2P3-LAPP, Annecy, France*
[9] *Université Clermont Auvergne, CNRS/IN2P3, LPC, Clermont-Ferrand, France*
[10] *Aix Marseille Univ, CNRS/IN2P3, CPPM, Marseille, France*
[11] *Université Paris-Saclay, CNRS/IN2P3, IJCLab, Orsay, France*
[12] *Laboratoire Leprince-Ringuet, CNRS/IN2P3, Ecole Polytechnique, Institut Polytechnique de Paris, Palaiseau, France*
[13] *LPNHE, Sorbonne Université Paris Diderot Sorbonne Paris Cité, CNRS/IN2P3, Paris, France*
[14] *I. Physikalisches Institut, RWTH Aachen University, Aachen, Germany*
[15] *Fakultät Physik, Technische Universität Dortmund, Dortmund, Germany*
[16] *Max-Planck-Institut für Kernphysik (MPIK), Heidelberg, Germany*
[17] *Physikalisches Institut, Ruprecht-Karls-Universität Heidelberg, Heidelberg, Germany*
[18] *School of Physics, University College Dublin, Dublin, Ireland*
[19] *INFN Sezione di Bari, Bari, Italy*
[20] *INFN Sezione di Bologna, Bologna, Italy*
[21] *INFN Sezione di Ferrara, Ferrara, Italy*
[22] *INFN Sezione di Firenze, Firenze, Italy*
[23] *INFN Laboratori Nazionali di Frascati, Frascati, Italy*
[24] *INFN Sezione di Genova, Genova, Italy*
[25] *INFN Sezione di Milano, Milano, Italy*
[26] *INFN Sezione di Milano-Bicocca, Milano, Italy*
[27] *INFN Sezione di Cagliari, Monserrato, Italy*

JHEP06(2023)132

[28] Università degli Studi di Padova, Università e INFN, Padova, Padova, Italy
[29] INFN Sezione di Pisa, Pisa, Italy
[30] INFN Sezione di Roma La Sapienza, Roma, Italy
[31] INFN Sezione di Roma Tor Vergata, Roma, Italy
[32] Nikhef National Institute for Subatomic Physics, Amsterdam, Netherlands
[33] Nikhef National Institute for Subatomic Physics and VU University Amsterdam, Amsterdam, Netherlands
[34] AGH - University of Science and Technology, Faculty of Physics and Applied Computer Science, Kraków, Poland
[35] Henryk Niewodniczanski Institute of Nuclear Physics Polish Academy of Sciences, Kraków, Poland
[36] National Center for Nuclear Research (NCBJ), Warsaw, Poland
[37] Horia Hulubei National Institute of Physics and Nuclear Engineering, Bucharest-Magurele, Romania
[38] Affiliated with an institute covered by a cooperation agreement with CERN
[39] ICCUB, Universitat de Barcelona, Barcelona, Spain
[40] Instituto Galego de Física de Altas Enerxías (IGFAE), Universidade de Santiago de Compostela, Santiago de Compostela, Spain
[41] Instituto de Fisica Corpuscular, Centro Mixto Universidad de Valencia - CSIC, Valencia, Spain
[42] European Organization for Nuclear Research (CERN), Geneva, Switzerland
[43] Institute of Physics, Ecole Polytechnique Fédérale de Lausanne (EPFL), Lausanne, Switzerland
[44] Physik-Institut, Universität Zürich, Zürich, Switzerland
[45] NSC Kharkiv Institute of Physics and Technology (NSC KIPT), Kharkiv, Ukraine
[46] Institute for Nuclear Research of the National Academy of Sciences (KINR), Kyiv, Ukraine
[47] University of Birmingham, Birmingham, United Kingdom
[48] H.H. Wills Physics Laboratory, University of Bristol, Bristol, United Kingdom
[49] Cavendish Laboratory, University of Cambridge, Cambridge, United Kingdom
[50] Department of Physics, University of Warwick, Coventry, United Kingdom
[51] STFC Rutherford Appleton Laboratory, Didcot, United Kingdom
[52] School of Physics and Astronomy, University of Edinburgh, Edinburgh, United Kingdom
[53] School of Physics and Astronomy, University of Glasgow, Glasgow, United Kingdom
[54] Oliver Lodge Laboratory, University of Liverpool, Liverpool, United Kingdom
[55] Imperial College London, London, United Kingdom
[56] Department of Physics and Astronomy, University of Manchester, Manchester, United Kingdom
[57] Department of Physics, University of Oxford, Oxford, United Kingdom
[58] Massachusetts Institute of Technology, Cambridge, MA, United States
[59] University of Cincinnati, Cincinnati, OH, United States
[60] University of Maryland, College Park, MD, United States
[61] Los Alamos National Laboratory (LANL), Los Alamos, NM, United States
[62] Syracuse University, Syracuse, NY, United States
[63] School of Physics and Astronomy, Monash University, Melbourne, Australia, associated to[50]
[64] Pontifícia Universidade Católica do Rio de Janeiro (PUC-Rio), Rio de Janeiro, Brazil, associated to[2]
[65] Physics and Micro Electronic College, Hunan University, Changsha City, China, associated to[7]
[66] Guangdong Provincial Key Laboratory of Nuclear Science, Guangdong-Hong Kong Joint Laboratory of Quantum Matter, Institute of Quantum Matter, South China Normal University, Guangzhou, China, associated to[3]
[67] School of Physics and Technology, Wuhan University, Wuhan, China, associated to[3]
[68] Departamento de Fisica, Universidad Nacional de Colombia, Bogota, Colombia, associated to [13]
[69] Universität Bonn - Helmholtz-Institut für Strahlen und Kernphysik, Bonn, Germany, associated to[17]
[70] Eotvos Lorand University, Budapest, Hungary, associated to[42]
[71] INFN Sezione di Perugia, Perugia, Italy, associated to[21]
[72] Van Swinderen Institute, University of Groningen, Groningen, Netherlands, associated to[32]
[73] Universiteit Maastricht, Maastricht, Netherlands, associated to[32]
[74] DS4DS, La Salle, Universitat Ramon Llull, Barcelona, Spain, associated to[39]

JHEP06(2023)132

[75] Department of Physics and Astronomy, Uppsala University, Uppsala, Sweden, associated to[53]
[76] University of Michigan, Ann Arbor, MI, United States, associated to[62]

[a] Universidade Federal do Triângulo Mineiro (UFTM), Uberaba-MG, Brazil
[b] Central South U., Changsha, China
[c] Hangzhou Institute for Advanced Study, UCAS, Hangzhou, China
[d] Excellence Cluster ORIGINS, Munich, Germany
[e] Universidad Nacional Autónoma de Honduras, Tegucigalpa, Honduras
[f] Università di Bari, Bari, Italy
[g] Università di Bologna, Bologna, Italy
[h] Università di Cagliari, Cagliari, Italy
[i] Università di Ferrara, Ferrara, Italy
[j] Università di Firenze, Firenze, Italy
[k] Università di Genova, Genova, Italy
[l] Università degli Studi di Milano, Milano, Italy
[m] Università di Milano Bicocca, Milano, Italy
[n] Università di Modena e Reggio Emilia, Modena, Italy
[o] Università di Padova, Padova, Italy
[p] Università di Perugia, Perugia, Italy
[q] Scuola Normale Superiore, Pisa, Italy
[r] Università di Pisa, Pisa, Italy
[s] Università della Basilicata, Potenza, Italy
[t] Università di Roma Tor Vergata, Roma, Italy
[u] Università di Siena, Siena, Italy
[v] Università di Urbino, Urbino, Italy
[†] Deceased

JHEP06(2023)132